Induced Stress Relationships for Wing Skin Forming by Shot Peening

R.D. VanLuchene, J. Johnson, and R.G. Carpenter

Shot peening has been used to provide fatigue resistance and form to airplane wing skins for many years. In the past, the peening intensities used to form these wing skins were obtained through the use of geometric relationships along with trial and error testing. A computer model was developed to model shot peening, which could eliminate the trial and error phases of the existing process. The computer model is used to determine the peening intensities across the wing skin and the initial size of the skin (flat pattern). To support such a computer model, we have developed in this paper relationships among the thickness of the material, the stress induced into the aluminum, and the intensity of the shot peening (shot wheel revolutions per minute, rpm). A simple induced stress theory is proposed. Results for a cylindrical wing skin utilizing the new relationships are included.

Keywords
shot, peening, induced, stress impirical

1. Introduction

IN ORDER to produce a method that can effectively improve on the techniques currently used to predict the peening intensities needed to form airplane wing skins, the fundamental effects of shot peening must be quantified. This paper describes the general effects that shot peening produces on a peened surface. The different machines that do the shot peening at the Boeing Commercial Airplane Company are also described.

The actual stresses induced by shot peening are approximated by simpler induced stress distributions that yield the same net effect as shot peening. These simplified induced stresses must be related to shot peen machine parameters and material properties. This is accomplished through a series of experimental tests relating geometric changes in peened specimens to theoretical equations. Through the use of these tests, relationships between the machine parameters and the simplified induced stress distributions are empirically derived.

1.1 *Shot Peening Behavior*

Shot peening is a process by which the surface of a metal part is repeatedly hit, at a high velocity, by small steel shot. Shot peening is used to induce surface residual compressive stresses in metal parts. The compressive stress improves the resistance of the metal to fatigue and stress corrosion cracking, which are a result of exposure to cyclical loads. Metal parts that are often shot peened are axles, springs, aircraft landing gear, and structural parts (Ref 1-4). Shot peening has been used recently to form thin metal parts, such as airplane wing skins. This process is called peen forming. Peen forming is performed by peening one or both sides of the part with varying intensities so that the part obtains a desired contoured shape.

When metal is shot peened, shot is propelled against the piece by means of large centrifugal wheels or by a stream of compressed air containing shot. The shot impacts the metal and forms a small indentation in the surface before bouncing off. The material around the indentation plastically deforms and flows out radially from the center of the indentation. Usually the piece of metal is peened until the surface becomes uniformly compacted.

Uniform peening produces a thin, plastically deformed layer with thickness, h_p, beneath the peened surface (Ref 2, 5, 6). Experimental results show that peening one side of a piece of metal and allowing the piece to reach equilibrium induces a stress distribution across the thickness similar to that shown in Fig. 1 (Ref 5, 6). The plastically deformed layer causes the metal to undergo several geometric changes in order to reach equilibrium. The top layer elongates (grows) in order to alleviate the compressive stress. The growth of this layer creates a growth differential across the specimen. This differential

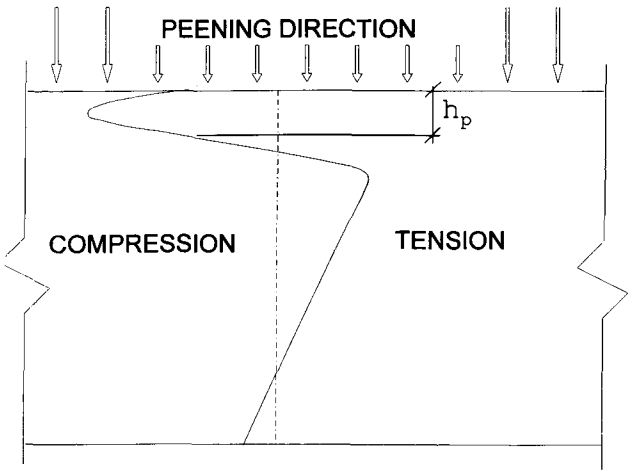

Fig. 1 Residual stress distribution after shot peening one side

R.D. VanLuchene and **J. Johnson,** Department of Civil Engineering, Montana State University, Bozeman, MT, USA; and **R.G. Carpenter,** Boeing Commercial Airplane Company, Seattle, WA, USA.

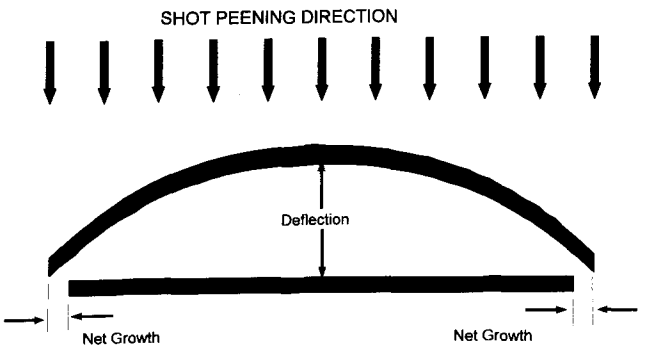

Fig. 2 Growth and curvature from shot peening on one side of a part

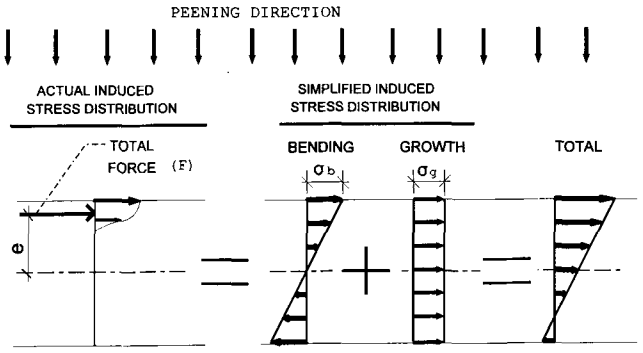

Fig. 3 Proposed shot peening equivalent induced stresses

causes the metal part to curve in the direction of the peened surface to maintain equilibrium as shown in Fig. 2 (Ref 7).

1.2 *Peening Equipment and Process Description*

The wing skin form peening equipment at the Boeing Commercial Airplane Company consists of three different machines: the spanwise, chordwise, and compression peening machines. The major differences between the spanwise and the chordwise machines are that the spanwise machine has larger shot size and the shot peening area or window is 18 in. wide by 3 in. high while the chordwise machine has a peening area of 18 in. by 18 in. The spanwise machine also achieves 100% coverage of shot impact while the chordwise machine achieves a 60% coverage. Percent coverage is defined as the percentage of the total surface area that has been impacted by shot during the peening process (Ref 8).

The spanwise machine is first used to form the skin. The sections of the skin that are spanwise peened are then sanded down to a specified smoothness in order to get rid of the large indentations made in the skin by the large size of the spanwise shot. The next step in the peen forming process is to run the skin through the chordwise peening machine. No sanding is required for the parts of the skin that are chordwise peened as a smaller shot size is used, which yields a relatively smooth surface.

After contour forming (spanwise and chordwise machines), wing skins are run through a third or compression peening machine, which has smaller shot size than either of the other machines. Compression peening is at 100% coverage across the entire skin. This protects the skin against fatigue cracking by putting a residual compressive layer on any section of the skin that is not peened with either the spanwise or chordwise machine.

1.3 *Limitations of the Present Method*

The present method for determining the peening pattern for a new aircraft wing skin has limitations. The initial flat shape (flat pattern) of the wing skin must be found before peening so that it ends up the correct size after it has undergone the growth and curvature associated with peening. The correct peening intensities must be obtained across the skin without trial and error. In the past at Boeing, the peening intensity pattern was modified numerous times before it was capable of accurately producing the desired shape with only one run through the peening machine. Several wing skins were commonly scrapped before an acceptable pattern was found. Under the old system, methods involving no knowledge of the intensity patterns were used to estimate the initial flat shape. This is clearly an oversight in method. The goal of the method developed herein is to convert the final shape of a wing skin into a flat pattern, which under the peening intensities predicted by the method, will form the aerodynamic shape of the wing skin.

2. Induced Stresses

2.1 *Equivalent Peening Stresses*

In order for shot peening to be modeled accurately, the modeling must account for the overall effects that shot peening produces in the material. Growth and curvature of the specimen, as seen in Fig. 2, must be capable of being developed by the model. If an aluminum specimen were rigidly constrained and then shot peened, a set of initial or induced stresses would be developed. If the specimen were then allowed to elastically deform into the shape of Fig. 2, the final residual stresses would be as shown in Fig. 1. The major thrust of this paper is to develop relationships for the initial or induced stresses. The term "induced" is used throughout and should not be confused with either the elastic recovery stresses or the residual stresses of Fig. 1. The induced stresses in the aluminum specimen are complicated and difficult to obtain. The effects that shot peening produces, however, can be achieved using a different and simpler set of stresses, as shown in Fig. 3.

The method developed for calculating peening intensities combines a finite element package along with sophisticated optimization software (FEM/OPT), which is proprietary to the Boeing Commercial Airplane Company. This method can predict the peening pattern and globally minimize the peening intensity needed to form a specific shape. The method calculates the total induced stress needed on the top, σ_{TOP}, and the bottom, σ_{BOT}, necessary for the correct shape to be formed. The stress distribution needed is defined by a straight line between the total stress at the top of the material, σ_{TOP}, and the total stress at the bottom of the material, σ_{BOT}. This stress distribution must be capable of being formed by the superposition of the simplified stress distribution due to peening the top of the material (see Fig. 3) and a similar simplified stress distribution due to

peening the bottom of the material. FEM/OPT calculates a value of σ_{TOP} and σ_{BOT} for each element used in the finite element mesh selected to model the wing skin.

Relationships among the simplified induced stresses of Fig. 3, the thickness of the material, and the peening intensity (shot wheel rpm) are needed in order to relate the stresses, σ_{TOP} and σ_{BOT}, calculated by FEM/OPT to shot peen machine parameters. This is accomplished by measuring laboratory specimens or coupons and developing the empirical relationships below.

2.2 *Development of Total Stress Equations*

Several coupons of different thicknesses were peened at varying intensities. Measurements of these coupons were used to determine the induced bending stress, σ_b, and the induced growth stress, σ_g, for peening on one side, using analytical equations. When one side of a coupon is peened, the total induced stress on the side that is peened will be $(\sigma_g + \sigma_b)$, and the induced stress on the side away from the peening will be $(\sigma_g - \sigma_b)$, as shown in Fig. 3. When both sides of the wing skin are peened (top and bottom), the total stress on the top of the skin, σ_{TOP}, can be obtained by superposition of the stresses induced by peening the top and bottom of the material:

$$\sigma_{TOP} = \sigma_{gT} + \sigma_{gB} + \sigma_{bT} - \sigma_{bB} \quad \text{(Eq 1)}$$

where σ_{gT} and σ_{gB} are the induced growth stresses due to peening on the top and bottom of the material, respectively, and σ_{bT} and σ_{bB} are the induced bending stresses caused by peening on the top and bottom of the material, respectively. Similarly, the total induced stress on the bottom of the wing skin, σ_{BOT}, will be:

$$\sigma_{BOT} = \sigma_{gT} + \sigma_{gB} + \sigma_{bB} - \sigma_{bT} \quad \text{(Eq 2)}$$

The growth stress, σ_g, for peening on one side may be described as a function of the bending stress, σ_b, for peening on the same side. A relationship between the bending stress, σ_b, and the growth stress, σ_g, is shown using Fig. 3. The growth stress, σ_g, in the simplified stress distribution is equal to the total force, F, given by the unknown actual induced stress distribution divided by the thickness of the material, t:

$$\sigma_g = \frac{F}{t} \quad \text{(Eq 3)}$$

The bending moment due to the actual stress distribution, M_{act}, is equal to the total force, F, multiplied by the moment arm, e, from the center of the material to the resultant of the induced stress distribution:

$$M_{act} = Fe \quad \text{(Eq 4)}$$

The moment due to the simplified induced stress distribution being used is:

$$M_{model} = \sigma_b t^2/6 \quad \text{(Eq 5)}$$

These two moments must be equal to one another in order for the simplified model to accurately depict what is happening during shot peening. Equations 4 and 5 lead to:

$$\sigma_b = 6Fe/t^2 \quad \text{(Eq 6)}$$

The ratio of σ_g to σ_b is then equal to:

$$\sigma_g/\sigma_b = t/(6e) \quad \text{(Eq 7)}$$

Since the compressed layer due to shot peening is very thin, e is approximately equal to one-half the thickness of the material; that is $e \approx t/2$. The ratio of σ_g to σ_b can then be approximated by:

$$\sigma_g/\sigma_b \approx \frac{1}{3} \quad \text{(Eq 8)}$$

Because the depth of the compressed layer is not infinitesimally small, e is actually smaller than one-half the thickness of the material. This will make the ratio of σ_g to σ_b slightly larger than 1/3.

The total required induced stresses, σ_{TOP} and σ_{BOT}, are produced by a finite element optimization program (FEM/OPT). A relationship of the form given by Eq 7 and 8 is also present between the induced growth stress, σ_g, and the induced bending stress, σ_b. This relationship along with Eq 1 and 2 will allow calculation of the two bending stresses, σ_{bT} and σ_{bB}. Once the induced bending stresses are known, it is possible to use a relationship described below to find the shot wheel rpm and the machine with which that section of the wing skin must be peened. The bending stress is being used to relate rpm to stress rather than the growth stress because the deformations that occur due to the bending stress are much larger and therefore easier to measure on a test coupon than the smaller deformations that occur due to the growth stress.

3. Experimental Procedure

3.1 *Peening Intensity versus Stress*

In order to relate the induced stress, which simulates the shot peening process, to the shot wheel rpm and the thickness of the material, 2.75 in. by 15.5 in. coupons of various thicknesses were shot peened at several peening intensities (shot wheel rpm). These thicknesses and intensities covered the range at which currently manufactured wing skins are peened. The test coupons were peened with a constant shot wheel rpm over the entire surface in order to obtain constant induced bending and growth stress.

Test coupons contain holes, which are drilled near both ends, to facilitate hanging the coupon on the racks, which carry the wing skins through the peening machines. The holes in the coupon were small enough that the effect they had on the results could be neglected. Rubber masking is placed on the back

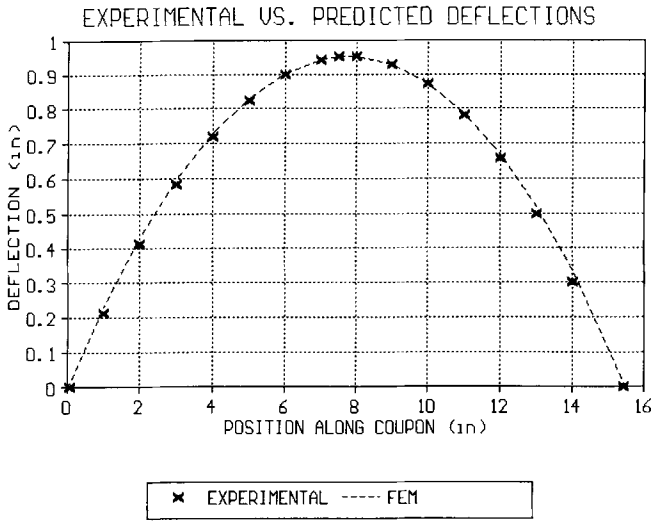

Fig. 4 Deflection of experimental coupon versus finite element deflection of a coupon with uniform bending stress

side of each coupon. This removes any accidental peening on the back side, which results from shot bouncing off the walls of the peening chamber.

A rectangular plate of length, L, width, W, and thickness, t, subjected to a constant induced bending stress in each direction, will have, according to thin plate theory, an elastic deflection at the center of the plate given as follows (Ref 9):

$$\Delta = \sigma_b(L^2 + W^2)(1 - \nu)/4Et \qquad \text{(Eq 9)}$$

Here σ_b is equal to the uniform bending stress in the plate as shown in Fig. 3, ν is Poisson's ratio of the material, and E is the modulus of elasticity. Equation 9 is valid for small deflections. This assumption may be violated in coupons peened at high wheel speeds. Some test coupons had as much as 1.5 in. of deflection over the 15.5 in. length. When large deflections are anticipated, the large deflection theory should be considered in order to determine the bending stress, σ_b.

Coupons that are peened with a constant intensity will also have a constant growth stress in both directions perpendicular to the peening direction. The induced growth stress, σ_g, present across a uniformly peened coupon will produce a growth strain, ε_g, given as follows (Ref 10):

$$\varepsilon_g = \sigma_g(1 - \nu)/E \qquad \text{(Eq 10)}$$

3.2 *Experimental Tests*

The induced bending stress, σ_b, predicted by Eq 9 was found for various peening intensities and thicknesses utilizing the deflection measured for each coupon. The equation that describes the intensity of the shot peening machine (rpm of shot wheel) as a function of the thickness of the material and the stress to be induced into the material is:

$$\text{rpm} = At^B\sigma_b^C \qquad \text{(Eq 11)}$$

where A, B, and C are constants obtained through a regression analysis. The form of this equation was chosen because it physically matches what happens during peening. If the machine intensity remains constant and the material gets thicker, the bending stress, σ_b, will go down due to the plastic layer reaching through a smaller percentage of the material. Similarly, if the bending stress, σ_b, increases while the material remains at a constant thickness, the rpm of the shot wheel must also go up to achieve a deeper plastic layer; that is, C must be a positive constant.

The accuracy of Eq 8 above was verified by equally peening on both sides. The growth strain, ε_g, (Eq 10), was found by measuring the length of the coupon after peening, subtracting the original length, and dividing by two, to obtain the growth for peening on one side. The growth stress was then found using Eq 10. To develop an empirical relationship between σ_b and σ_g, these stresses were compared for the same rpm of shot peen wheel and thickness for the spanwise machine. Equation 12 shows the empirical relationship chosen:

$$\sigma_g = A\sigma_b \qquad \text{(Eq 12)}$$

where A is a constant obtained through a regression analysis. The form of this equation was chosen due to an observation that the ratio of the growth to bending stress was constant for all thicknesses as predicted by Eq 8.

3.3 *Multiple Peening Machine Considerations*

The coupons that are peened with each of the three machines must be treated differently in order to obtain an induced stress that accurately models what is going on when a skin is peened by all three in a combined fashion. The coupons peened with the spanwise machine are sanded down to certain smoothness specifications to which actual wing skins must adhere. Coupon measurements of deflection and growth are therefore taken after the sanding has been performed. The sanding reduces both the deflection and the growth due to a loss of part of the plastically deformed compressive layer during sanding.

As noted above, the sections of a skin that are shot peened with the chordwise machine only have a 60% coverage. When a skin is compression peened, the remaining 40% is peened. This leads to higher induced stresses in these sections than if chordwise peening acted alone. Therefore, when a coupon is measured for chordwise peening, it must also be compression peened on the same side that it is chordwise peened to account for the increase in stress.

The compression peening machine produced coupons that could be measured without further processing. The compression peening machine test coupons are needed in order to obtain the minimum induced stress values for σ_g and σ_b. These minimum induced values are used by FEM/OPT during the calculation of σ_{TOP} and σ_{BOT}.

3.4 *Experimental Results*

The deflected shapes of several of the uniformly peened coupons were compared to the deflected shape of a finite element model, subject to uniform bending, to ensure that the peened coupons were behaving as though a bending stress acted uniformly

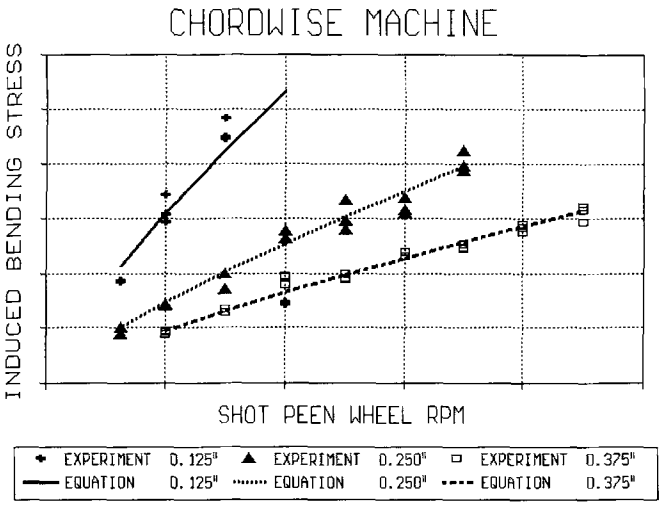

Fig. 5 Chordwise machine: bending stress as a function of shot peen wheel rpm

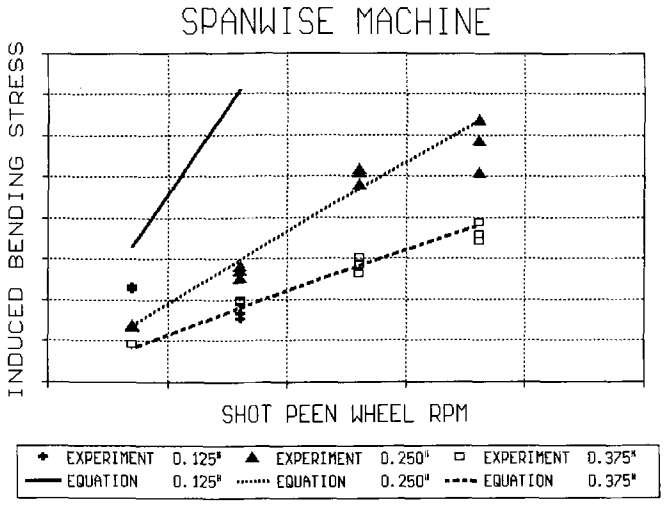

Fig. 6 Spanwise machine: bending stress as a function of shot wheel rpm

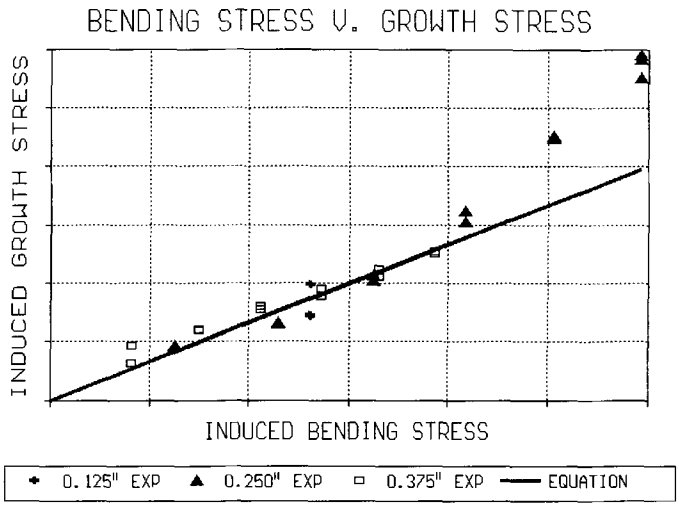

Fig. 7 Growth stress as a function of bending stress

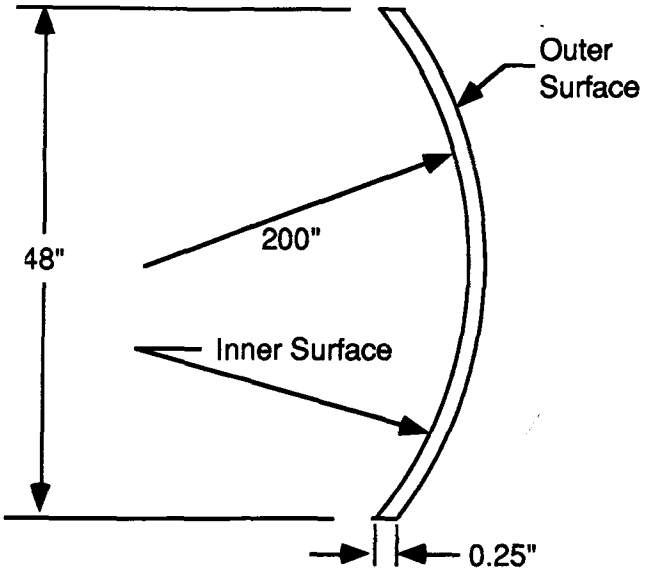

Fig. 8 Target cylindrical shape

across the coupon. Deflections measured along the long axis of a typical coupon and the finite element solution with the same deflection are shown in Fig. 4. The agreement between the finite element shape and the actual shape of the test coupons was convincing evidence that uniform peening does induce a uniform bending stress.

When the constants for Eq 11 were calculated for both the spanwise and the chordwise machines, the shape of the equation closely matched the experimental data, as shown in Fig. 5 and 6.

The tendency for the induced bending stress, σ_b, to increase with wheel rpm is not observed in the relatively thin 0.125 in. plates above a certain intensity. This is due to the plastically deformed layer in the coupon producing stresses that decrease the overall bending moment. Once the plastic layer reaches a depth near the middle of the coupon, the bending moment begins to decrease. Further peening decreases the moment. Intensities past the peak bending stress are not requested by the FEM/OPT program. Neglecting high intensities with thin coupons leads to the maximum stresses being low with thin specimens, reaching a maximum in specimens with an average thickness, and going down as the thickness of the specimens increases from the average.

The coefficient for Eq 12 was 0.366 for the spanwise machine data using a regression analysis. This value is close to the limiting value of 1/3 predicted by Eq 8. No growth data were available for either the chordwise machine or the compression machine. Because the intensities of these two machines are less than the intensity of the spanwise machine, the compressive layer logically will be thinner. Then, the ratio of σ_g to σ_b will approach the limiting 1/3 value for these machines. Figure 7 shows a line that depicts the 1/3 value running through the spanwise data. This value fits well for the lower intensities on the spanwise machine. Data at high intensities that deviate

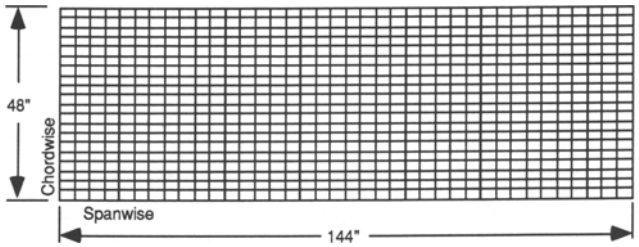

Fig. 9 Input analysis mesh

from the 1/3 value are rarely used due to rough surface resulting from these intensities. The 1/3 value for the coefficient in Eq 12 therefore appears acceptable for all peening intensities that are used in FEM/OPT.

4. Verification of Results Using a Test Skin

4.1 *Purpose*

The purpose of this test was to investigate the accuracy of the FEM/OPT software using the equations developed herein for predicting the shot peening patterns necessary for forming contoured surfaces, such as wing skins. A cylindrical section was selected as the contoured surface to test. Generating a cylinder from a rectangular plate presents a challenge due to the similarity between its required shot pattern and that of the easier to generate pattern of the spherical shape. A spherical shape usually results when a plate is subjected to a constant magnitude blast over its entire surface. A cylinder, on the other hand, usually results from a pattern that has a slightly higher magnitude peening along the outer edges than it does down the center of the plate. The test was structured to peen a cylindrical shape along the short (chordal) length of the coupons with no curvature along the long (span) length.

4.2 *Procedure*

The test started as a computer-aided design (CAD) model of a 48 in. by 144 in. by 0.25 in. cylindrical section curved along the short (48 in.) side. The cylindrical section was given a 200 in. radius, as shown in Fig. 8. The preprocessor to FEM/OPT allows control over the number of rows and columns of elements in a grid. For this test, a grid with 20 rows and 38 columns was constructed. This resulted in a mesh of 760 elements having an element size of 2.40 in. by 3.78 in. Figure 9 shows the resulting mesh. FEM/OPT also allows the selection of the maximum peen wheel rpm for the inner and outer surface peening both chordwise and spanwise machines. For both tests, an 800 rpm maximum was specified for chordwise inner and chordwise outer peening. No peening was specified for the spanwise peen machine. Once modeling was complete, the analysis portion of FEM/OPT was executed using the generated input files. The results were then plotted using the postprocessor of FEM/OPT, and the resulting peen output files were manually converted to numerical control (NC) instructions. Figure 10 shows the peen pattern predicted by the software.

Study of the pattern shows distinct symmetry, which is expected for a cylindrical section. Since the output is based on a

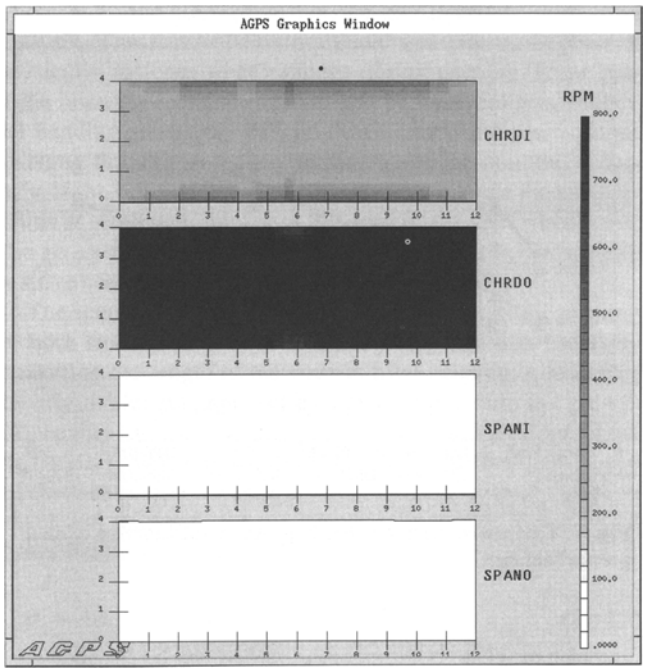

Fig. 10 Predicted peening pattern

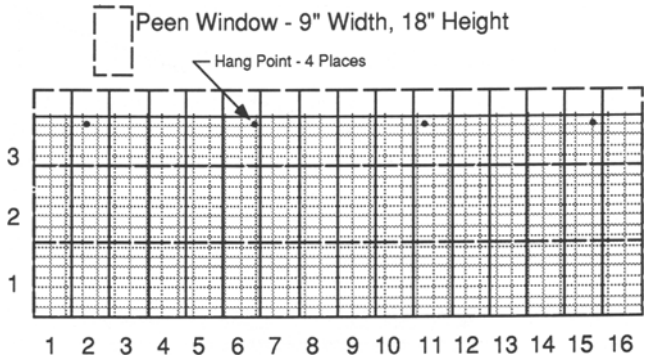

Fig. 11 Peen grid overlaying analysis grid

rather fine resolution (2.40 in. by 3.78 in. element size) grid, it had to be converted to the coarser resolution (18 in. by 9 in.) grid on which the peen machine is based. Figure 11 shows the peen grid (dashed lines) overlaying the analysis grid. All peen values that fall within a given peen window are averaged, and this single value is used in the NC instructions to control the peening. A source of error is possible at this stage, so care must be taken to ensure that the requested peening values are accurately converted to NC instructions.

After the averaged peen values are converted to NC instructions, the instructions are down loaded to the shop floor peen machine controller. The coupons are prepared for peening by mounting them onto the overhead rail system that feeds the panel through the peen machine. Mounting is at four attachment points, as shown in Fig. 11. The mounts are tightly clamped down to suppress any relative motion between the coupon and the rail system.

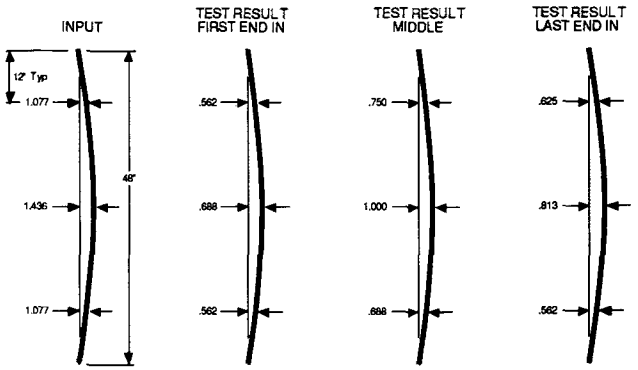

Fig. 12 Comparison of chordal results

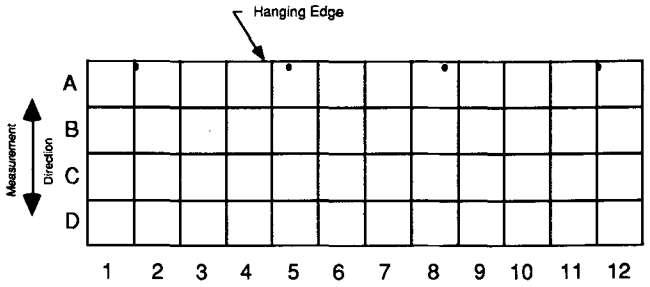

Fig. 13 Results of the radius of curvature measurements for the coupon

Table 1 Chord height error: input versus measured

	Input, in.	Test results, in. First end in	Middle	Last end in	Errors, % First end in	Middle	Last end in
Top	1.077	0.562	0.750	0.625	48	30	42
Center	1.436	0.688	1.000	0.813	52	30	43
Bottom	1.077	0.562	0.688	0.562	48	36	48
Equivalent radius	200	417	287	352			

4.3 *Results*

A dial indicator gage with data recorder was used to gather data at 48 points on the surface of the peened test coupon. Also, a series of 9 chord height measurements were recorded using a straight edge and steel rule. Figure 12 shows the results of the chord height measurements along with a comparison of the target input chord heights. Table 1 shows the percentage error at each of the 9 measurement points when compared to the values of the target. Figure 13 and corresponding Table 2 show the results of the radius of curvature measurements for the coupon.

On the basis of the results shown in Tables 1 and 2, the coupon was underpeened. In general, the goal of the test was to produce a cylindrical shape that was without serious rippling or waviness. There were no expectations to produce a shape that exactly matched the input. A study of the chord height measurements and the radius of curvature measurements easily shows that the shape is fairly well behaved.

One of the problems with this test was that the material database used was for 2324 aluminum alloy, whereas the tests were conducted using 2024 alloy (due to easy availability of 2024). This mismatch in materials caused some difference in the resulting curvature. Another problem was that the measurements were taken as the coupons hung vertically from the overhead rail system, rather than on a horizontal test fixture. This caused the radius measurements to appear larger than actual, due to the effects of gravity tending to straighten the hanging coupon. This will give the impression of underpeening. Neither of these two problems will account for the errors that these tests produced. The software should produce better results when using the correct material database and a measurement test fixture along with other refinements in FEM/OPT.

5. Conclusion

Form peening is a process that has been modeled by inadequate methods in the past. Through the use of finite element modeling procedures and experimental data analysis, the process of arriving at the peening intensities necessary to form a specific shape can be greatly improved. This new method uses a simplified induced stress model. The induced stresses are capable of providing the same net effects that shot peening produces. Empirical relationships can be derived for the parameters that control shot peening intensities, material properties, and the resulting induced stresses. The relationships allow for a simple and accurate method to determine shot peening patterns. A full scale test has been run using FEM/OPT and the equations developed herein on a cylindrical panel with positive results.

Acknowledgments

R.D. VanLuchene and J. Johnson gratefully acknowledge the Boeing Commercial Airplane Group for the knowledge, time, material, and support that they so graciously gave.

References

1. U.S. Army Laboratory Command, "Shot Peening of Metal Parts," Military Specification, MIL-S-13165C
2. ASM Committee on Shot Peening, "Shot Peening," *Metals Handbook*, 9th ed., Vol 5, American Society for Metals, 1982, p 138-149
3. *Mechanical Engineer's Handbook*, John Wiley & Sons, 1986, p 942-951
4. D.V. Nelson, R.E. Ricklefs, and W.P. Evans, The Role of Residual Stresses in Increasing Long-Life Fatigue Strength of Notched

Table 2 Radius of curvature results

Column	Radius, in. A	B	C	D
1	547	514	363	279
2	954	477	405	365
3	723	422	369	388
4	585	373	304	318
5	540	372	282	281
6	336	362	305	269
7	347	343	267	262
8	462	351	303	275
9	479	358	338	357
10	710	423	529	347
11	539	529	478	364
12	355	354	415	371
Average	548	407	363	323
Error	174%	104%	82%	62%

Average radius = 410 in.
Standard deviation = 134 in.
Minimum radius = 262 in.
Maximum radius = 954 in.

Machine Members, *Achievement of High Fatigue Resistance in Metals and Alloys*, STP 467, ASTM, 1970, p 228-253

5. S.T.S. Al-Hassani, Mechanical Aspects of Residual Stress Development in Shot Peening, *Proceedings of the First International Conference on Shot Peening* (Paris), Pergamon Press, Sept 1981, p 583-602

6. S.T.S. Al-Hassani, The Shot Peening of Metals—Mechanics and Structures, *Shot Peening for Advanced Aerospace Design*, SP-528, Society of Automotive Engineers, 1982, p 23-28

7. S.E. Homer and R.D. VanLuchene, Aircraft Wing Skin Contouring by Shot Peening, *J. Mater. Shaping Technol.*,Vol 9, No2, 1991, p 1-13

8. P.G. Feld and D.E. Johnson, Advanced Concepts of the Process, *Shot Peening for Advanced Aerospace Design*, SP-528, Society of Automotive Engineers, 1982, p 19-22

9. S. Timoshenko and S. Woinowsky-Kreiger, *Theory of Plates and Shells*, 2nd ed., McGraw-Hill, 1959, p 33-43

10. S.P. Timoshenko and J.N. Goodier, *Theory of Elasticity*, 3rd ed., McGraw-Hill , 1970, p 8-9